Highlighted paper selected by Editor-in-chief

Cytoprotective Effects of KIOM-79 on Streptozotocin Induced Cell Damage by Inhibiting ERK and AP-1

Kyoung Ah KANG,[a] Kyoung Hwa LEE,[a] So Young KIM,[b] Hee Sun KIM,[b] Jin Sook KIM,[c] and Jin Won HYUN*,[a]

[a] *Department of Biochemistry, College of Medicine and Applied Radiological Science Research Institute, Cheju National University; Jeju-si 690–756, Korea:* [b] *Department of Neuroscience, College of Medicine, Ewha Womans University; Seoul 110–783, Korea: and* [c] *Department of Herbal Pharmaceutical Development, Korea Institute of Oriental Medicine; Daejeon 305–811, Korea.* Received October 20, 2006; accepted January 30, 2007

The present study investigated the potential cytoprotective properties of a combination of plant extracts (KIOM-79) obtained from *Magnolia officinalis*, *Pueraria lobata*, *Glycyrrhiza uralensis*, and *Euphorbia pekinensis*, against the oxidative stresses induced by streptozotocin (STZ) in a rat pancreatic β-cells (RINm5F). KIOM-79 was found to scavenge intracellular reactive oxygen species (ROS), thereby preventing DNA damage and lipid peroxidation. The KIOM-79 inhibited apoptosis of the β-cells exposed to STZ *via* radical scavenging activity and activation of antioxidant enzymes. KIOM-79 inhibited activation of extracellular regulated kinase (ERK) induced by STZ and inhibited DNA binding activity of an activator protein-1 (AP-1), a downstream transcription factor of ERK. Taken together, these findings suggest that KIOM-79 protects against STZ induced cell death in RINm5F cells by inhibiting ROS generation and the ERK pathway.

Key words cytoprotective property; KIOM-79; reactive oxygen species; oxidative stress

Oxidative stress is suggested as a mechanism underlying the complications of diabetes.[1)] Reactive oxygen species (ROS) have been implicated in the pathology of various disease states, including diabetes mellitus and it is well known that superoxide anion is the radical formed by the reduction of molecular oxygen that may lead to ROS such as hydrogen peroxide and hydroxyl radical.[1,2)] In the streptozotocin (STZ)-induced rat diabetes model, an activated oxygen species was proposed to be formed and involved in the death of the β-cells.[3)] STZ (*N*-(methyl nitro carbamoyl)-D-glucosamine) is a potent DNA methylating agent and acts as a free radical donor in the pancreas where the β-cells are particularly sensitive to damage from free radicals because of a low level of free radical scavenging enzymes.[4,5)]

Medicinal plants are currently being investigated for their pharmacological properties in the regulation of blood glucose and apoptosis induced by oxidative stress, a process which is pivotal in the pathology of diabetes mellitus.[6,7)] A combination of plant extracts (KIOM-79) was prepared from *Magnolia officinalis*, *Pueraria lobata*, *Glycyrrhiza uralensis*, and *Euphorbia pekinensis*. *Magnolia officinalis* reportedly has antimutagenic,[8)] hepatocytic protective,[9,10)] neuroprotective,[11)] and anti-inflammatory effects.[12)] *Pueraria lobata* reportedly has antimutagenic, antidiabetic and antioxidant effects.[13—15)] *Glycyrrhiza uralensis* has detoxification, antiulcer, antiinflammation, antiviral, antiatherogenic, and anticarcinogenic effects,[16)] and *Euphorbia pekinensis* has for antiviral and cytotoxic activities.[17,18)] Recently, KIOM-79 has suggested possible anti-inflammatory properties by blocking NFκB/Rel and p38 kinase activation.[19)]

We have investigated the protective effects of KIOM-79 on oxidative stress induced by STZ in this study of the pancreatic β-cells and the likely cytoprotective mechanism.

MATERIALS AND METHODS

Preparation of KIOM-79 The cortex of *Magnolia officinalis*, radix of *Pueraria lobata*, radix of *Glycyrrhiza uralensis*, and radix of *Euphorbia pekinensis* were collected from plants obtained from the province Gamsuk (China) and identified by Professor J. H. Kim, Division of Life Science, Daejeon University. All voucher specimens have been deposited at the herbarium of the Department of Herbal Pharmaceutical Development, Korea Institute of Oriental Medicine (No. 1240, 2, 7, and 207, respectively). Magnoliae cortex (100 g) was simmered with 3 g of Zingiberis rhizomes for 60 min. Puerariae radix (100 g) was stir-roasted at 75 °C for 45 min and when the radix surface yellowed with brown spots, it was removed and allowed to cool. An equal amount of gingered Magnoliae cortex, parched Puerariae radix, Glycyrrhizae radix, and Euphoriae radix was mixed, pulverized, extracted in 80% ethanol for one week at room temperature, concentrated with a rotary evaporator, and lyophilized, and the entire procedure was repeated for four times.

Cell Culture RINm5F rat pancreatic β-cells obtained from the American Type Culture Collection were maintained at 37 °C in an incubator with a humidified atmosphere of 5% CO_2 and cultured in RPMI-1640 medium containing 10% heat-inactivated fetal calf serum, streptomycin (100 μg/ml) and penicillin (100 units/ml).

Intracellular Reactive Oxygen Species (ROS) Measurement and Image Analysis The DCF-DA method was used to detect intracellular ROS levels.[20)] DCF-DA diffuses into cells where it is hydrolyzed by intracellular esterase to a polar 2′,7′-dichlorodihydrofluorescein moiety. This non-fluorescent fluorescein analog gets trapped within the cells and is oxidized by intracellular oxidants to 2′,7′-dichlorofluorescein, which is highly fluorescent. The RINm5F cells were treated with the KIOM-79 preparation at concentrations of 10, 50, and 100 μg/ml for 1 h and STZ (10 mM) was then added. The cells were incubated for an additional 24 h at 37 °C. After the addition of 25 mM of DCF-DA solution, the fluorescence of 2′,7′-dichlorofluorescein was detected using a Perkin Elmer LS-5B spectrofluorometer, confocal laser mi-

* To whom correspondence should be addressed. e-mail: jinwonh@cheju.ac.kr

croscope, and assessed using a flow cytometer (Becton Dickinson, Mountain View, CA, U.S.A.), respectively. For the image analysis of the production of intracellular ROS, RINm5F cells were seeded in cover slip-loaded 6 well plates at 1×10^5 cells/ml. At 16 h after plating, the cells were treated with KIOM-79 for 30 min followed by the addition of STZ (10 mM) to the plates. After a media change, 100 μM of DCF-DA was added to the well and incubation continued for an additional 30 min at 37 °C. After washing with PBS, stained cells were mounted onto microscope slide using mounting medium (DAKO, Carpinteria, CA, U.S.A.). Images were collected using a Laser Scanning Microscope 5 PASCAL program (Carl Zeiss) on a confocal microscope.

Western Blot Cells were placed in a culture dish at 1×10^6 cells/dish and at 16 h after plating, the cells were treated with KIOM-79 at 50 μg/ml. The cells were harvested, and washed twice with PBS. The harvested cells were lysed on ice for 30 min in 100 μl of a lysis buffer [120 mM NaCl, 40 mM Tris (pH 8), 0.1% NP 40] and centrifuged at $13000\times\boldsymbol{g}$ for 15 min. Supernatants were collected from the lysates and protein concentrations determined. Aliquots of the lysates (40 μg of protein) were boiled for 5 min and electrophoresed in 10% sodium dodecysulfate-polyacrylamide gel. Gels were transferred onto nitrocellulose membranes (Bio-Rad), which were then incubated with primary antibodies. The membranes were further incubated with secondary immunoglobulin-G-horseradish peroxidase conjugates (Pierce). Protein bands were detected using an enhanced chemiluminescence Western blotting detection kit (Amersham) and then exposed to X-ray film.

Immunocytochemical Analysis Cells plated on cover slips were fixed with 4% paraformaldehyde for 30 min and permeabilized with 0.1% Triton X-100 in PBS for 2.5 min. Cells were then treated with a blocking medium (3% bovine serum albumin in PBS) for 1 h and further incubated with anti-phosphor histone H2A.X antibody diluted in blocking medium for 2 h. Immunoreactive primary phosphor histone H2A.X antibody was detected by a 1 : 500 dilution of FITC-conjugated secondary antibody (Jackson ImmunoResearch Laboratories) for 1 h. After washing with PBS, the stained cells were mounted onto microscope slides in mounting medium with DAPI (Vector). Images were collected using the Laser Scanning Microscope 5 PASCAL program (Carl Zeiss) on a confocal microscope.

Lipid Peroxidation Assay Lipid peroxidation was assayed by the thiobarbituric acid (TBA) reaction.[21] The cells were seeded in a culture dish at 1×10^6 cells/dish. At 16 h after plating, the cells were treated with 50 μg/ml of KIOM-79 and 1 h later, 10 mM STZ was added to the plate and incubated for further 1 h. The cells were then washed with cold PBS, scraped and homogenized in ice-cold 1.15% KCl. One hundred microliters of the cell lysates was mixed with 0.2 ml of 8.1% sodium dodecylsulfate, 1.5 ml of 20% acetic acid (adjusted to pH 3.5) and 1.5 ml of 0.8% thiobarbituric acid. The mixture was made up to a final volume of 4 ml with distilled water and heated at 95 °C for 2 h. After cooling to room temperature, 5 ml of *n*-butanol and pyridine mixture (15 : 1, v/v) was added to each sample, and the mixture was shaken. After centrifugation at $1000\times\boldsymbol{g}$ for 10 min, the supernatant fraction was isolated, and the absorbance measured spectrophotometrically at 532 nm. The amount of thiobarbituric acid reactive substance (TBARS) was determined using standard curve of 1,1,3,3-tetrahydroxypropane.

Cell Viability The effect of STZ on the viability of the RINm5F cells was determined using the [3-(4,5-dimethylthiazol-2-yl)-2,5-diphenyltetrazolium]bromide (MTT) assay, which is based on the reduction of a tetrazolium salt by mitochondrial dehydrogenase in the viable cells.[22] The RINm5F cells were treated with KIOM-79 and STZ, and the cells were incubated for 24 h at 37 °C. Fifty microliters of the MTT stock solution (2 mg/ml) was then added to each well for a total reaction volume of 200 μl. After incubating for 4 h, the plate was centrifuged at $800\times\boldsymbol{g}$ for 5 min and the supernatants were aspirated. The formazan crystals in each well were dissolved in 150 μl of DMSO and the A_{540} was read on a scanning multi-well spectrophotometer.

Nuclear Staining with Hoechst 33342 The cells were placed in a 24 well plate at 2×10^5 cells/well. At 16 h after plating, the cells were treated with 50 μg/ml of KIOM-79 and after further incubation for 1 h, 10 mM STZ was added to the culture. After 24 h, 1.5 μl of Hoechst 33342 (stock 10 mg/ml), a DNA specific fluorescent dye, was added to each well (1.5 ml) and incubated for 10 min at 37 °C. The stained cells were then observed under a fluorescent microscope, which was equipped with a CoolSNAP-Pro color digital camera, to examine the degree of nuclear condensation.

DNA Fragmentation For detection of DNA fragmentation, the cells were placed in a culture dish at 1×10^6 cells/dish. At 16 h after plating, the cells were treated with 50 μg/ml of KIOM-79. After a further incubation for 1 h, 10 mM STZ was added to the culture, and the cells harvested after 24 h. Cellular DNA-fragmentation was assessed by analysis of the cytoplasmic histone-associated DNA fragmentation using Roche diagnostics kit according to the manufacturer's instructions. A Comet assay was performed to assess oxidative DNA damage.[23,24] Cell pellets (1.5×10^5 cells) were mixed with 100 μl of 0.5% low melting agarose (LMA) at 39 °C and spread on fully frosted microscope slides that were pre-coated with 200 μl of 1% normal melting agarose (NMA). After agarose solidification, the slides were covered with another 75 μl of 0.5% LMA and then immersed in lysis solution (2.5 M NaCl, 100 mM Na-EDTA, 10 mM Tris, 1% Trion X-100, and 10% DMSO, pH 10) for 1 h at 4 °C. The slides were then placed in a gel-electrophoresis apparatus containing 300 mM NaOH and 10 mM Na-EDTA (pH 13) for 40 min to allow DNA to unwind and the expression of the alkali labile damage. An electrical field was applied (300 mA, 25 V) for 20 min at 4 °C to draw negatively charged DNA toward the anode. After electrophoresis, the slides were washed three times for 5 min at 4 °C in a neutralizing buffer (0.4 M Tris, pH 7.5) and then stained with 75 μl of ethidium bromide (20 μg/ml). The slides were examined using a fluorescence microscope and image analysis (Komet). The percentage of total fluorescence in the tail and tail lengths of at least 50 cells per slide were recorded.

8-Hydroxy-2′-deoxyguanosine (8-OHdG) Assay 8-OHdG amount in DNA was determined using Bioxytech 8-OHdG-ELISA Kit purchased from OXIS Health Products following the manufacturer's instructions. Cellular DNA was isolated using DNAzol reagent (Life Technologies) and quantified using a spectrophotometer.

Antioxidant Enzymes Activity The cells were seeded at

1×10^5 cells/ml, and at 16 h after plating, the cells were treated with KIOM-79 for 3 h. The harvested cells were suspended in 10 mM phosphate buffer (pH 7.5) and then lysed on ice by sonication twice for 15 s. Triton X-100 (1%) was then added to the lysates which was further incubated for 10 min on ice. The lysates were centrifugated at 5000×***g*** for 30 min at 4 °C to remove the cellular debris and the protein content was determined. For detection catalase activity, 50 μg of protein was added to 50 mM phosphate buffer (pH 7) containing 100 mM (v/v) H_2O_2. The reaction mixture was incubated for 2 min at 37 °C and absorbance monitored at 240 nm for 5 min. Changes in absorbance with time was proportional to the breakdown of H_2O_2.[25] Catalase activity was expressed as units/mg protein where one unit of enzyme activity was defined as the amount of enzyme required to breakdown of 1 μM H_2O_2. For detection of superoxide dismutase activity, Fifty micrograms of the protein was added to 500 mM of the phosphate buffer (pH 10.2) containing 0.1 mM EDTA and 0.4 mM epinephrine. Epinephrine rapidly undergoes auto-oxidation at pH 10 to produce adrenochrome, which is a pink colored product, measured at 480 nm using a UV/VIS spectrophotometer in kinetic mode. Superoxide dismutase inhibits the auto-oxidation of epinephrine. The rate of inhibition was monitored at 480 nm and one unit of enzyme activity was defined as the amount of enzyme required to produce 50% inhibition of enzyme activity. The superoxide dismutase activity is expressed as units/mg protein. For detection of glutathione peroxidase activity, 50 μg of the protein was added to 25 mM of the phosphate buffer (pH 7.5), 1 mM EDTA, 1 mM NaN_3, 1 mM glutathione, 0.25 unit of glutathione reductase, and 0.1 mM NADPH. After incubation for 10 min at 37 °C, H_2O_2 was added to the reaction mixture at a final concentration of 1 mM. The absorbance was monitored at 340 nm for 5 min. The glutathione peroixdase activity was measured as the rate of NADPH oxidation at 340 nm. The glutathione peroixdase activity is expressed as units/mg protein.

Preparation of Nuclear Extract and the Electrophoretic Mobility Shift Assay The cells were placed in a culture dish at 1×10^6 cells/dish. At 16 h after plating, the cells were treated with 50 μg/ml of KIOM-79. After a further incubation for 3 h, 10 mM STZ was added to the culture and after 3 h, the cells were harvested, and lysed on ice with 1 ml of lysis buffer (10 mM Tris–HCl, pH 7.9, 10 mM NaCl, 3 mM $MgCl_2$, and 1% NP-40) for 4 min. After 10 min of centrifugation at 3000×***g***, the pellets were resuspended in 50 μl of extraction buffer (20 mM HEPES, pH 7.9, 20% glycerol, 1.5 mM $MgCl_2$, 0.2 mM EDTA, 1 mM DTT, and 1 mM PMSF), incubated on ice for 30 min, and centrifuged at 13000×***g*** for 5 min. The supernatant (nuclear protein) was stored at −70 °C after determination of protein concentration. Oligonucleotides containing the transcription factor AP-1 consensus sequence (5′-CGC TTG ATG ACT CAG CCG GAA-3′) were annealed, labeled with [γ-^{32}P] ATP using T4 polynucleotide kinase, and used as probes. The probes (50000 cpm) were incubated with 6 μg of the nuclear extracts at 4 °C for 30 min in a final volume of 20 μl containing 12.5% glycerol, 12.5 mM HEPES (pH 7.9), 4 mM Tris–HCl (pH 7.9), 60 mM KCl, 1 mM EDTA, and 1 mM DTT with 1 μg of poly (dI-dC). Binding products were resolved on 5% polyacrylamide gel and the bands visualized by autoradiography. For competition binding assays, binding reaction reagents and nuclear extracts were mixed with nonradioactive oligonucleotides in molar excess and incubated before adding ^{32}P-labeled probe. For supershift assay, antibody was coincubated with the nuclear extract mix for 30 min on ice prior to addition of the radiolabeled probe. Antibodies against c-Jun and c-Fos were purchased from Santa Cruz Biotechnology.

Statistical Analysis All the measurements were made in triplicate and all values were represented as means±standard error. The results were subjected to an analysis of the variance (ANOVA) using the Tukey test to analyze the differences. A value of $p<0.05$ was considered to be significant.

RESULTS

ROS Scavenging Activity of KIOM-79 The scavenging effects of KIOM-79 on intracellular ROS were investigated. The intracellular ROS scavenging activity of KIOM-79 was 36% at 10 μg/ml, 52% at 50 μg/ml, and 55% at 100 μg/ml (Fig. 1A). ROS levels were detected using flow cytometry (Fig. 1B) and showed 227 value of fluorescence intensity produced from ROS stained by DCF-DA fluorescence dye in STZ treated cells with KIOM-79, compared to 251 value of fluorescence intensity in the STZ treated cells. The fluorescence intensity of DCF-DA staining was enhanced in the STZ treated RINm5F cells as shown in Fig. 1C. KIOM-79 reduced the red fluorescence intensity upon STZ treatment, reflecting a reduction in ROS generation. These data, therefore, suggest that KIOM-79 has ROS scavenging activity.

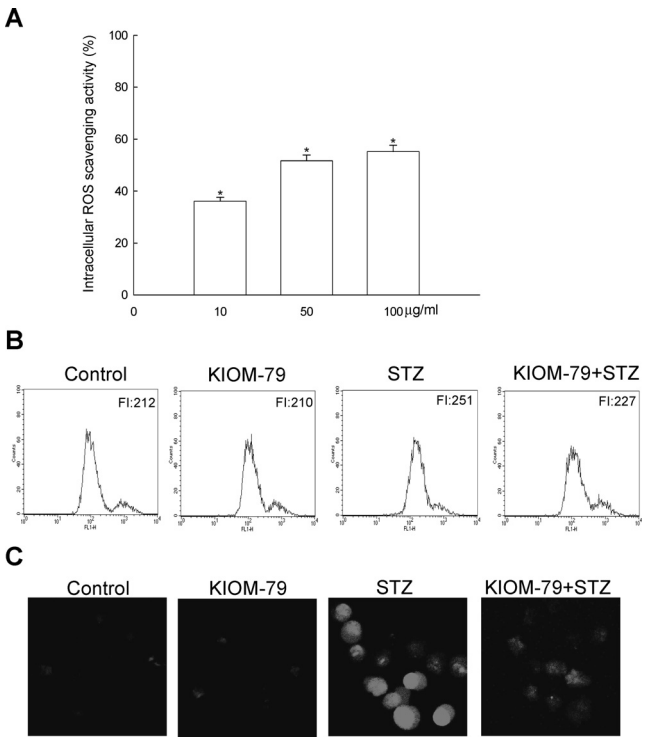

Fig. 1. Effects of KIOM-79 on Intracellular ROS

The intracellular ROS generated was detected using the DCF-DA method (A) and flow cytometry analysis (B). (C) Representative confocal images illustrate the increase in red fluorescence intensity of DCF produced by ROS in STZ treated cells as compared to control and the lowered fluorescence intensity in STZ treated cells exposed to KIOM-79 (original magnification ×400). The measurements were made in triplicate and values are expressed as means±standard error.

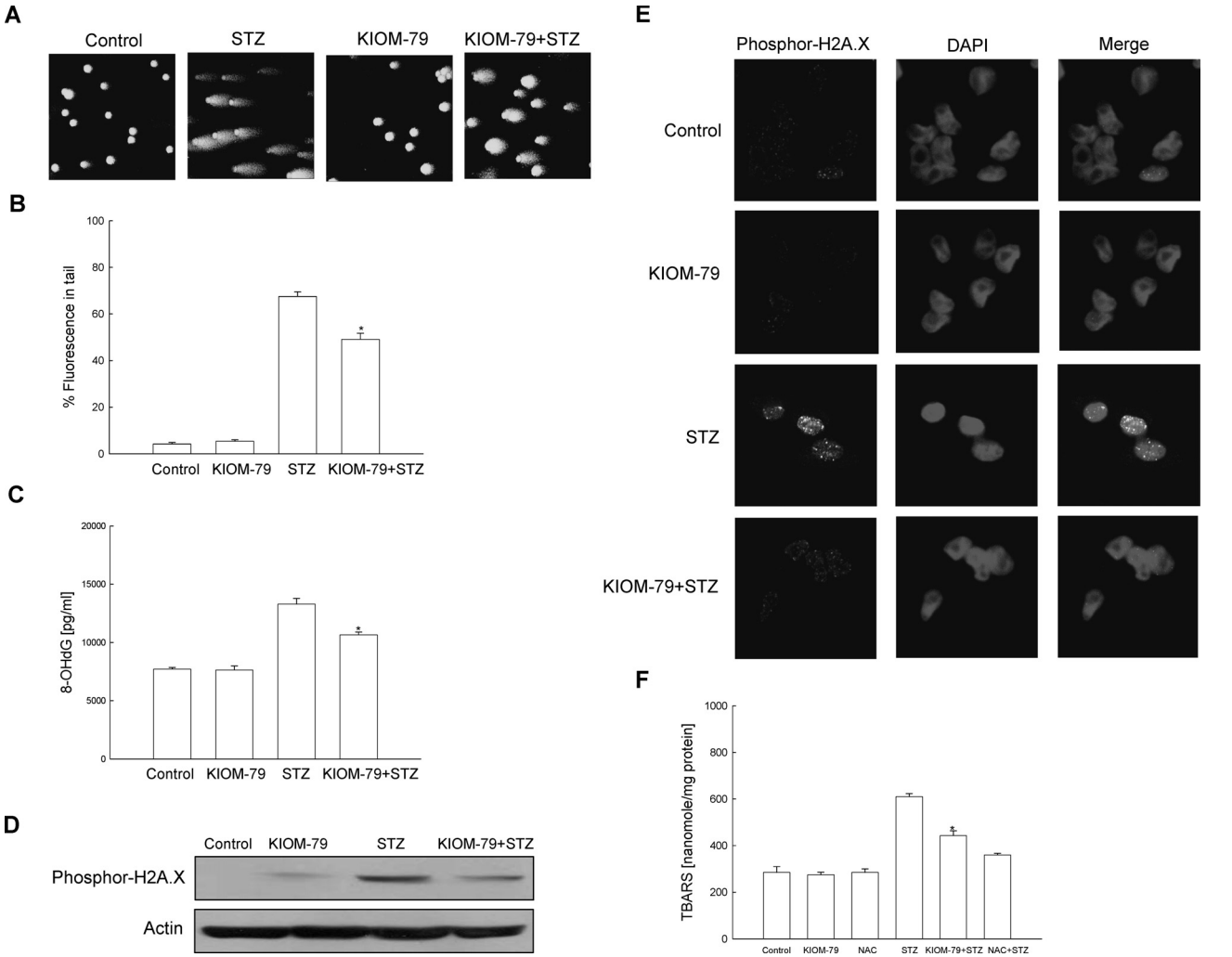

Fig. 2. Effects of KIOM-79 on DNA Damage and Lipid Peroxidation

(A) Representative images and (B) the percentage of cellular DNA damage detected by an alkaline comet assay. ∗Significantly different from STZ treated cells ($p<0.05$). (C) 8-OHdG content in cellular DNA measured in ELISA kit. ∗Significantly different from STZ treated cells ($p<0.05$). (D) Cell lysates were electrophoresed and phosphor H2A.X protein was detected using a specific antibody. (E) The confocal image indicates that FITC-conjugated secondary antibody staining identifies the location of phosphor H2A.X (green) by anti-phosphor H2A.X antibody, DAPI staining indicates the location of the nucleus (blue), and the merged image indicates the location of the phosphor H2A.X protein in nucleus. (F) Lipid peroxidation was assayed by measuring the amount of TBARS formation. Measurements were made in triplicate and the values expressed as means±standard error. ∗Significantly different from STZ treated cells ($p<0.05$).

Effects of KIOM-79 on Cellular DNA Damage and Lipid Peroxidation Induced by STZ The abilities of KIOM-79 on cellular DNA damage and membrane lipid peroxidation in STZ treated cells were investigated. Damage to cellular DNA induced by STZ exposure was detected by using an alkaline comet assay and assessing phosphor histone-H2A.X expression. The exposure of cells to STZ increased the parameters of tail length and percentage of DNA in the tails of the cells. When the cells were exposed to STZ, the percent of DNA in the tail increased 68%, and treatment with KIOM-79 resulted in a decrease to 49% as shown in Figs. 2A and B. 8-OHdG adduct in DNA has been used most extensively as a biomarker of oxidative stress.[26] As shown in Fig. 2C, STZ treatment increased 13290 pg/ml of 8-OHdG amount compared to 7710 pg/ml in control cells, and KIOM-79 treatment decreased 10650 pg/ml, indicating a protective effect of KIOM-79 on STZ induced DNA damage. In addition, the phosphorylation of nuclear histone H2A.X, a sensitive marker for breaks of double stranded DNA,[27] increased in the STZ treated cells as shown by western blot and immuno-fluorescence analyses (Figs. 2D, E). However, KIOM-79 in STZ treated cells decreased the expression of phosphor histone H2A.X, thereby indicating a protective effect of KIOM-79 on STZ induced DNA damage. STZ induced damage to cell membrane underlies the loss of cell viability through the peroxidation of membrane lipids. As shown in Fig. 2F, RINm5F cells exposed to STZ have an increase of 610 nmol/mg protein in TBARS of lipid peroxidation compared to 285 nmol/mg protein in control group. KIOM-79, however, decreased 443 nmol/mg protein of the STZ induced lipid peroxidation. *N*-Acetylcystein (NAC) as a positive control decreased 360 nmol/mg protein of the STZ induced lipid peroxidation.

Effects of KIOM-79 on Cell Death Induced by STZ The potential protective effects of KIOM-79 on cell survival in the STZ treated cells were evaluated. Cells were treated with KIOM-79 at 50 μg/ml for 1 h, prior to the addition of STZ. Cell viability was determined 24 h later by the MTT assay. As shown in Fig. 3A, KIOM-79 treatment of the STZ exposed cells increased survival by 65% as compared to 34%

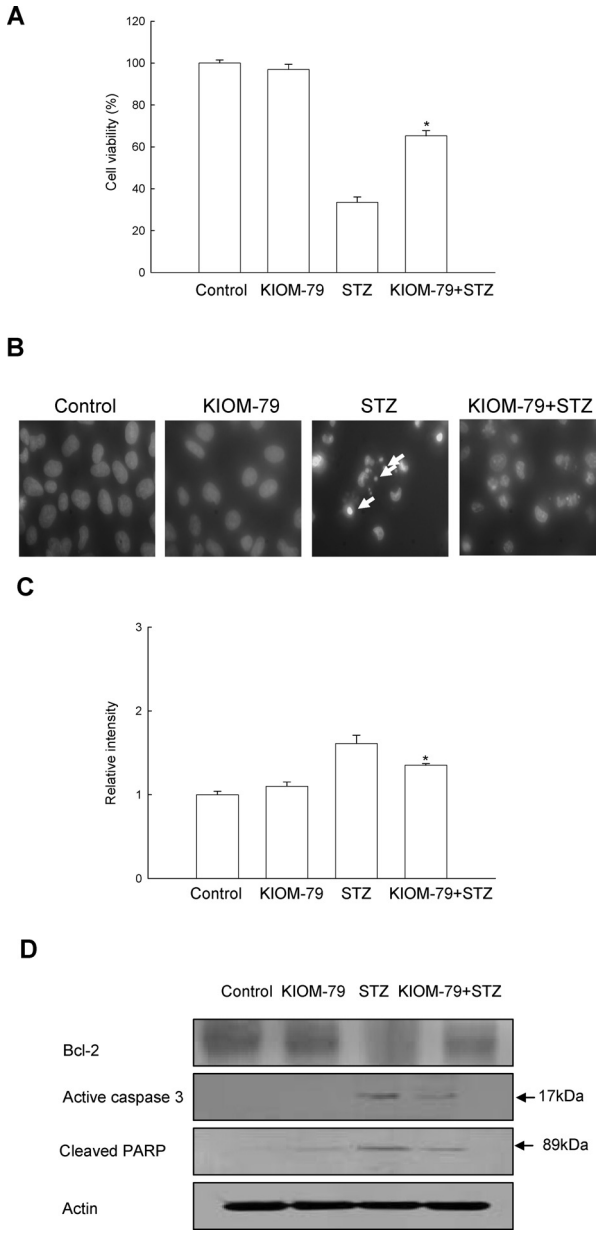

Fig. 3. Protective Effects of KIOM-79 on STZ Induced Cell Damage

(A) The viability of RINm5F cells following STZ treatment was determined by MTT assay. (B) Apoptotic body formation was observed under a fluorescent microscope after Hoechst 33342 staining Apoptotic bodies are indicated by arrows. (C) DNA fragmentation was quantified by ELISA kit. Measurements were made in triplicate and values expressed as means±standard error. * Significantly different from STZ treated cells ($p<0.05$). (D) Cell lysates were electrophoresed and the expressions of Bcl-2, caspase 3 and PARP were detected by its specific antibody.

determined for STZ treatment alone. To further evaluate the potential cytoprotective effects of KIOM-79 on apoptosis induced by STZ, the nuclei of RINm5F cells were stained with Hoechst 33342 and assessed by microscopy. Figure 3B indicates that control cells had intact cell nuclei, while STZ treated cells showed significant nuclear fragmentation, characteristic of apoptosis, whereas, cells treated with KIOM-79 1 h prior to STZ treatment, evinced a decrease in nuclear fragmentation. In addition to the morphological evaluation, the protective effect of KIOM-79 against apoptosis was also confirmed by ELISA based quantification of cytoplasmic histone-associated DNA fragmentation. As shown in Fig. 3C, treatment of cells with STZ increased the levels of cytoplasmic histone-associated DNA fragmentations compared to control group, however, treatment with 50 μg/ml of KIOM-79 decreased the STZ induced level of DNA fragmentation. To understand how KIOM-79 protects STZ induced apoptosis, we examined changes of Bcl-2 and caspase 3 activity by western blot. As shown in Fig. 3D, the Bcl-2, an anti-apoptotic protein, was recovered in KIOM-79 and STZ treated cells compared to STZ treated cells. One of the actions of Bcl-2 during the apoptotic process is to prevent the opening of mitochondrial membrane pore.[28] It is suggested that pore opening induces the disruption of mitochondrial membrane potential, which in turn lead to the release of cytochrome *c* from mitochondria, and finally induce apoptosis *via* caspases cascade.[29] It was also observed the decreased activation of caspase 3 (17 kDa), the major effecter caspase of the apoptotic process, and PARP cleavage (89 kDa), one of substrates of activated caspase 3, in combination with KIOM-79 and STZ compared to STZ treatment. These results suggest, therefore, that KIOM-79 provides a protective role for cell viability by inhibiting STZ induced apoptosis.

Effects of KIOM-79 on Antioxidant Enzymes To investigate whether the radical scavenging activity of KIOM-79 was mediated by the activities of antioxidant enzymes, the activities of catalase, superoxide dismutase, and glutathione peroxidase in the KIOM-79 treated RINm5F cells were measured. KIOM-79 increased the activities of these three enzymes (Fig. 4A); in the catalase activity, 13 U/mg protein at 50 μg/ml compared to 6 U/mg protein of the control; in the superoxide dismutase activity, 23 U/mg protein at 50 μg/ml compared to 15 U/mg protein of the control; in the glutathione peroxidase activity, 26 U/mg protein at 50 μg/ml compared to 18 U/mg protein of the control. The induction of catalase by KIOM-79, in terms of protein expression, was confirmed by western blot analysis. As shown in Fig. 4B, the treatment of KIOM-79 increased the protein expression of catalase within 6 h. In addition, KIOM-79 increased the catalase activity decreased by STZ treatment (Fig. 4C).

Effects of KIOM-79 on STZ Induced ERK and AP-1 Activation We examined the effects of KIOM-79 on the activation of ERK, JNK, and p38 in STZ treated cells. The activation states of ERK, JNK, and p38 were determined using phosphorylated antibodies. Cells were pretreated with 50 μg/ml of KIOM-79 for 1 h and then treated with 10 mM of STZ for 3 h. The KIOM-79 was found to prevent the activation of ERK, but had no effect on the activation of JNK and p38 by STZ, and the total expressions of the ERK, JNK, and p38 remained unchanged (Fig. 5A). The AP-1 transcription factor consists of either homodimeric or heterodimeric complexes including c-Jun or c-Fos family members. It has been reported that ERK activation leads to c-Fos phosphorylation, which constitutes the AP-1.[30] AP-1 is a downstream target of the phospho-ERK pathway and activated AP-1 is involved in cell death.[31] Therefore, we examined the effect of KIOM-79 on the DNA binding activity of AP-1. As shown in Fig. 5B, treatment of cells with STZ increased AP-1 activation while KIOM-79 inhibited STZ induced AP-1 activity. Competition assay revealed that the complex is AP-1-specific, since it was diminished by molar excess of cold oligonucleotide of its own AP-1 (AP-1) but not by other non-specific oligonucleotide (NF-κB) (Fig. 5B, middle panel). Moreover, a supershift assay indicated that the AP-1 complex is composed of

c-Fos and c-Jun subunits because the complex was supershifted by antibodies against c-Fos or c-Jun protein. Taken together, these results suggest that KIOM-79 inhibits STZ induced cell death by suppressing both ERK and AP-1 activation.

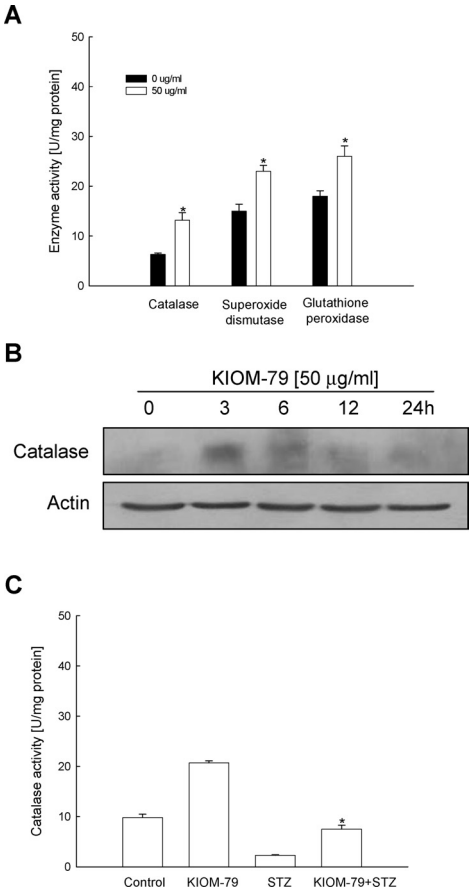

Fig. 4. Effects of KIOM-79 on Antioxidant Enzymes

(A) The enzyme activity is expressed as average enzyme units per mg protein±standard error. * Significantly different from control ($p<0.05$). (B) Cell lysates treated with 50 μg/ml of KIOM-79 were electrophoresed and the expression of catalase was detected by catalase specific antibody. (C) The catalase activity is expressed as average enzyme units per mg protein±standard error. * Significantly different from STZ treated cells ($p<0.05$).

DISCUSSION

This study demonstrates that KIOM-79 protects pancreatic β-cells from STZ induced cell death. Whereas STZ induced the release of ROS, KIOM-79 attenuated this effect, suggesting KIOM-79 to have antioxidant properties. STZ stimulates ROS release which is speculated to result in diabetes mellitus.[3] Most evidence supporting this possibility was obtained from *in vitro* and *in vivo* studies, in which STZ increased free radical production, lipid peroxidation, and DNA damage in β-cells, and radical scavengers such as metallothionein, melatonin, quercetin, superoxide dismutase, and vitamin E reduced the severity of the STZ induced oxidative damage.[32—38] In the present study, KIOM-79 was found to decrease intracellular ROS levels, cellular DNA damage, and the lipid peroxidation that is induced by STZ. The cells exposed to STZ exhibited the distinct morphological features of apoptosis, including morphological changes and DNA fragmentation. Cells pretreated with KIOM-79, however, had a significant reduction in the percentage of apoptotic cells. These findings suggest that KIOM-79 inhibits STZ induced apoptosis through an ROS scavenging effect. Catalase, superoxide dismutase, and glutathione peroxidase play significant roles in effectively augmentation of antioxidant cellular defense mechanisms. KIOM-79 increased these enzymes activity, suggesting that the scavenging of ROS by KIOM-79 may be related to increased antioxidant activity. Diabetic pancreas showed decreased activities of key antioxidant enzymes and the level of nonenzymic antioxidants.[39] KIOM-79 augmented the catalase activity decreased by STZ treatment in RINm5F cells, suggesting that KIOM-79 may be scavenge the ROS generated by STZ treatment. To further analyze a molecular mechanism underlying the inhibitory effect on apoptosis by KIOM-79, we investigated the mitogen activated protein kinases (MAPK) family and AP-1 signaling pathway. STZ treatment induced a phosphor form of the ERK, JNK, and p38 MAPK. KIOM-79 was observed to decrease the expression of a phosphor ERK protein, but did not change activation of JNK, and p38. The other research group reported that KIOM-79 inhibited iNOS gene expression by blocking of phosphorylation of p38 kinase.[19] These different effects of KION-79 on inhibiting of p38 activity might contribute to be differently the *in vitro* system used. The activa-

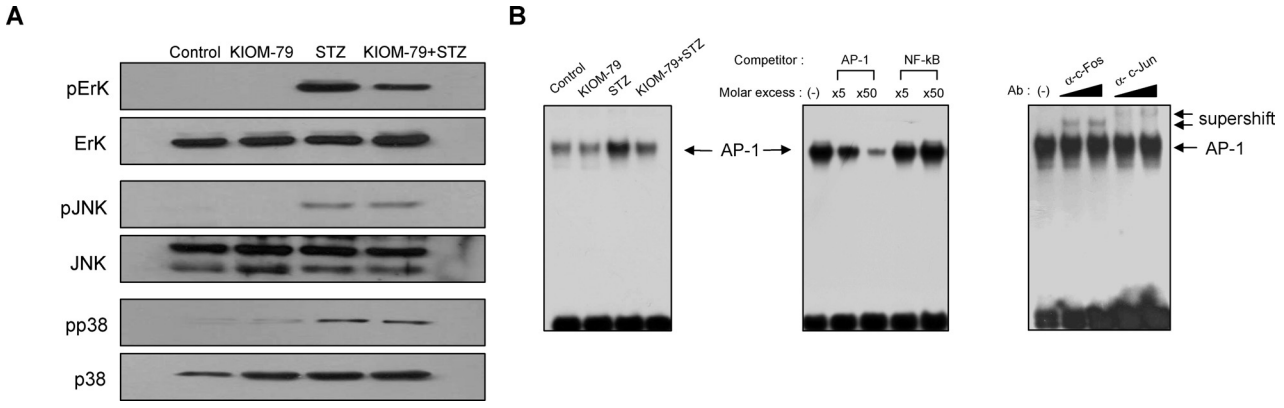

Fig. 5. Effects of KIOM-79 on STZ Induced ERK and AP-1 Activation

(A) Cell lysates were electrophoresed and gels were immunoblotted using antibodies against phospho- and total form of MAP kinases. (B) EMSA for AP-1 DNA binding activity. Nuclear extracts were prepared from RINm5F cells after treatment with KIOM-79 for 3 h in the absence or presence of STZ. The arrow indicates a DNA–protein complex of AP-1 (left panel). Competition assay (middle panel) and supershift assay (right panel) indicate that the complex is AP-1-specific.

tion of ERK was suggested to be a critical components in the oxidative stress induced apoptosis process.[40] Activated ERK can induce c-Fos, which is a component of AP-1.[41] Previous studies have demonstrated that AP-1 is an important regulator of proliferation, transformation, and apoptosis, depending on the cell type.[42,43] An electrophoretic mobility shift analysis revealed that an increase in the DNA binding activity of AP-1 induced by STZ was inhibited by KIOM-79, and suggesting that the AP-1 pathway may be involved in the protective effect of KIOM-79 on cell apoptosis. Our results, threrfore, indicate that inhibition of ERK by KIOM-79 down-regulates the activation of the AP-1 transcription factor.

In conclusion, we have provided evidence that KIOM-79, a combination of plant extracts, attenuates the STZ induced cell apoptosis process through the inhibition of ROS generation and the ERK/AP-1 signaling pathway in the pancreatic β-cells.

Acknowledgements This research was supported by a grant [L06010] from the Korea Institute of Oriental Medicine.

REFERENCES

1) Halliwell B., Gutteridge J. M. C., "Free Radicals in Biology and Medicine," 2nd ed., Oxford University Press, Oxford, 1989.
2) Baynes J. W., *Diabetes*, **40,** 405—412 (1991).
3) Schmezer P., Eckert C., Liegibel U. M., *Mutat. Res.*, **307**, 495—499 (1994).
4) Lukic M. L., Stosic-Grujicic S., Shahin A., *Dev. Immunol.*, **6**, 119—128 (1998).
5) Spinas G. A., *News Physiol. Sci.*, **14**, 49—54 (1999).
6) Kinloch R. A., Treherne J. M., Furness L. M., Hajimohamadreza I., *Trends Pharmacol. Sci.*, **20**, 35—42 (1999).
7) Latha M., Pari L., Sitasawad S., Bhonde R., *J. Biochem. Mol. Toxicol.*, **18**, 261—272 (2004).
8) Saito J., Sakai Y., Nagase H., *Mutat. Res.*, **609**, 68—73 (2006).
9) Park E. J., Kim S. Y., Zhao Y. Z., Sohn D. H., *Planta Med.*, **72**, 661—664 (2006).
10) Cao A. H., Vo L. T., King R. G., *Phytother. Res.*, **19**, 932—937 (2005).
11) Lin Y. R., Chen H. H., Ko C. H., Chan M. H., *Eur. J. Pharmacol.*, **537**, 64—69 (2006).
12) Lee J., Jung E., Park J., Jung K., Lee S., Hong S., Park J., Park E., Kim J., Park S., Park D., *Planta Med.*, **71**, 338—343 (2005).
13) Miyazawa M., Sakano K., Nakamura S., Kosaka H., *J. Agric. Food Chem.*, **49**, 336—341 (2001).
14) Lee K. T., Sohn I. C., Kim D. H., Choi J. W., Kwon S. H., Park H. J., *Arch. Pharm. Res.*, **23**, 461—466 (2000).
15) Lee K. T., Sohn I. C., Kim Y. K., Choi J. H., Choi J. W., Park H. J., Itoh Y., Miyamoto K., *Biol. Pharm. Bull.*, **24**, 1117—1121 (2001).
16) Wang Z. Y., Nixon D. W., *Nutr. Cancer*, **39**, 1—11 (2001).
17) Ahn M. J., Kim C. Y., Lee J. S., Kim T. G., Kim S. H., Lee C. K., Lee B. B., Shin C. G., Huh H., Kim J., *Planta Med.*, **68**, 457—459 (2002).
18) Kong L. Y., Li Y., Wu X. L., Min Z. D., *Planta Med.*, **68**, 249—252 (2002).
19) Jeon Y. J., Li M. H., Lee K. Y., Kim J. S., You H. J., Lee S. K., Sohn H. M., Choi S. J., Koh J. W., Chang I. Y., *J. Ethnopharmacol.*, **108**, 38—45 (2006).
20) Rosenkranz A. R., Schmaldienst S., Stuhlmeier K. M., Chen W., Knapp W., Zlabinger G. J., *J. Immunol. Meth.*, **156**, 39—45 (1992).
21) Ohkawa H., Ohishi N., Yagi K., *Anal. Biochem.*, **95**, 351—358 (1979).
22) Carmichael J., DeGraff W. G., Gazdar A. F., Minna J. D., Mitchell J. B., *Cancer Res.*, **47**, 936—941 (1987).
23) Singh N. P., *Mutat. Res.*, **455**, 111—127 (2000).
24) Rajagopalan R., Ranjan S. K., Nair C. K., *Mutat. Res.*, **536**, 15—25 (2003).
25) Carrillo M. C., Kanai S., Nokubo M., Kitani K., *Life Sci.*, **48**, 517—521 (1991).
26) Toraason M., Clark J., Dankovic D., Mathias P., Skaggs S., Cynthia W., Werren D., *Toxicology*, **138**, 43—53 (1999).
27) Rogakou E. P., Pilch D. R., Orr A. H., Ivanova V. S., Bonner W. M., *J. Biol. Chem.*, **273**, 5858—5868 (1988).
28) Zamzami N., Marchetti P., Castedo M., Zanin C., Vayssiere J. L., Petit P. X., Kroemer G., *J. Exp. Med.*, **181**, 1661—1672 (1995).
29) Zamzami N., Susin S. A., Marchetti P., Hirsch T., Gomez-Monterrey I., Castedo M., Kroemer G., *J. Exp. Med.*, **183**, 1533—1544 (1996).
30) Murakami M., Ui M., Iba H., *Cell Growth Differ.*, **10**, 333—342 (1999).
31) Kitamura M., Ishikawa Y., Moreno-Manzano V., Xu Q., Konta T., Lucio-Cazana J., Furusu A., Nakayama K., *Nephrol. Dial. Transplant.*, **17**, 84—87 (2002).
32) Coskun O., Kanter M., Korkmaz A., Oter S., *Pharmacol. Res.*, **51**, 117—123 (2005).
33) Eum W. S., Choung I. S., Li M. Z., Kang J. H., Kim D. W., Park J., Kwon H. Y., Choi S. Y., *Free Radic. Biol. Med.*, **37**, 339—349 (2004).
34) Bolzan A. D., Bianchi M. S., *Mutat. Res.*, **512**, 121—134 (2002).
35) Szkudelski T., *Physiol. Res.*, **50**, 537—546 (2001).
36) Chen H., Carlson E. C., Pellet L., Moritz J. T., Epstein P. N., *Diabetes*, **50**, 2040—2046 (2001).
37) Andersson A. K., Sandler S., *J. Pineal. Res.*, **30**, 157—165 (2001).
38) Vannucchi H., Araujo W. F., Bernardes M. M., Jordao Junior A. A., *Int. J. Vitam. Nutr. Res.*, **69**, 250—254 (1999).
39) Latha M., Pari L., Sitasawad S., Bhonde R., *J. Biochem. Molecular Toxicol.*, **18**, 261—272 (2004).
40) Ishikawa Y., Kitamura M., *Kidney Int.*, **58**, 1078—1087 (2000).
41) Whitmarsh A. J., Davis R. J., *J. Mol. Med.*, **74**, 589—607 (1996).
42) Brown P. H., Alani R., Preis L. H., Szabo E., Birrer M. J., *Oncogene*, **8**, 877—886 (1993).
43) Liebermann D. A., Gregory B., Hoffman B., *Int. J. Oncol.*, **12**, 685—700 (1998).